COBEM 2021 26th International Congress of Mechanical Engineering
November 22-26, 2021, Virtual Congress, Brazil

COB-2021-2275
IMPACT OF VISCOSITY ON BLOOD FLOW IN ASCENDING AORTIC ANEURYSM

Gabriela de Castro Almeida
Bruno Nieckele Azevedo
Julia de Almeida Silva
Ivan Fernney Ibanez
Bruno Alvares de Azevedo
Angela O. Nieckele
Pontifícia Universidade Católica do Rio de Janeiro, Department of Mechanical Engineering, 22451-900, Rio de Janeiro, RJ, Brazil
gabrielacastro@aluno.puc-rio.br, bruno.n.azevedo@gmail.com, jusilva1597@gmail.com, iibanez@puc-rio.br, azevedo@puc-rio.br, nieckele@puc-rio.br

Fabiula Schwartz Azevedo
Glaucia Maria Moraes de Oliveira
Universidade Federal do Rio de Janeiro, Department of Internal Medicine, Faculty of Medicine,21044-020, Rio de Janeiro, RJ, Brazil
fabiulaschwartz@gmail.com, glauciamoraesoliveira@gmail.com

Abstract. *Blood viscosity is established by several factors such as blood cell distribution, mechanical properties and/or percentage of red blood cells on the total volume of the blood. This last factor is known as hematocrit level. Higher the hematocrit rate, higher the blood viscosity. Understanding the consequences of the blood rheology in the flow field and how it can affect the vascular health is essential to help the diagnosis and treatment of patients that have different types of diseases. The identification of the impacts of different viscosities in the flow field in a realistic aorta geometry is important since measurement of the blood viscosity is a challenge, and its accurate value may not be available. Further, it can help to understand the correlation between blood factors and how it can affect possible pathologies in arteries. In the present work, the particular interest is related to patients with ascending aortic aneurysm, and how the flow structures can be correlated with the aneurysm growth or not. In this way, this research compares the flow in the major artery of the human body – the aorta – corresponding to two distinct years of two patients, one with aneurysm growth and the other without growth, considering the blood as a Newtonian fluid with two different viscosities (3.5cP and 7.2cP) and as a non-Newtonian fluid with 3.5cP limiting viscosity, using the Carreau model. The aorta dimensional model was generated by the segmentation of computed tomography angiograph images. Using Computer Fluid Dynamics, the flow is obtained with a commercial software, ANSYS Fluent. The most critical condition corresponding to the maximum flow rate during the systole period is considered. Due to the high flow rate, and large vessel diameter, the flow behaves as turbulent and it was solved with the RANS methodology employing the two-equation κ-ω SST turbulence model. It was observed a small impact of the blood rheology in the flow field. Similar wall shear stress distribution was also observed, although the viscosity presented a direct influence on its level.*

Keywords. *blood viscosity, CFD, hemodynamic, aorta*

1. INTRODUCTION

Blood is a body fluid responsible to deliver necessary substances to the cell and transports waste products to be discarded. It has a complex structure, being composed by plasma and red blood cells, white blood cells and platelets. The rheological behavior of blood can be characterized by the viscosity shear rate dependency. It is a relevant parameter to characterize the blood, with direct impact in its circulation, since its variation can impair the normal flow. It can occur as a result of different factors, such as blood cells distribution, mechanical properties or percentage of red blood cells on the total volume of the blood, namely as hematocrit level.

When viscosity is independent of the fluid deformation rate, the fluid is classified as Newtonian fluid, otherwise as non-Newtonian fluid. The approximation of the blood as a Newtonian fluid is commonly considered (Yamamoto et al., 2020) when the deformation rate varies above 50 s^{-1} (Long et al., 2004; Crowley & Pizziconi, 2005). It reduces the non-linearity of the momentum equation, leading to easier, cheaper and faster numerical solution. Blood viscosity is hard to measure, and values from 2.5 cP to 8 cP can be found in the literature. Becsek et al. (2020) evaluated different values of blood viscosity and demonstrated negligible effect on the mean flow field and a very small effect on the location of the turbulent breakdown. The values investigated were 4 cP, 6 cP and 8 cP.

The study of the flow pattern along the ascending aorta has been presented by several authors (Gomes et al., 2017, Celis et al., 2020, Ibanez et al., 2020, Johnson et al., 2020, Bessa et al., 2021) aiming to understand the impact of the flow

in the tension distribution over the aortic wall. Recently, Almeida et al. (2021) investigated the flow pattern in aortas of nine patients with aortic aneurysms, based on exams of two different years, and discussed that the angle between the direction of the blood jet entering the ascending aorta can induce flow recirculation in the posterior area, increasing pressure level at the aortic wall, what might lead to aneurysm growth.

Based on the impact that viscosity might have on the flow, in the present work, the viscosity behavior as non-Newtonian and Newtonian fluid with different viscosities is investigated, with focus of its impact in patients with aorta aneurysm. To this end, two patients with ascending aortic aneurysm are analyzed, considering two different years of computed tomography angiography (CTA) exams for each patient.

2. METHODOLOGY

CTA exams were used for the creation of the patient's geometry. From these CTA series, DICOM (Digital Imaging and Communication in Medicine) images were transferred to Mimics (Materialise, Belgium) software and then the segmentation was performed by FIJI (open source image processing software based on ImageJ), making it possible to create the three dimensional (3D) model. This research was approved by the ethics committee of the National Institute of Cardiology, INC/MS.

For this study, it was considered the flow during the peak of the ventricular systole (twenty-five liters per minute), that is the period that occurs the maximum physiological flow rate. At this moment, the aortic walls are distended, providing the maximum diameter, with small variation due the vascular complacency. Thus, aorta's surface was defined as rigid, due its small complacency (Viscardi et al., 2010). Gravity effects are neglected, since the pressure variations are dominant, and under normal conditions, blood density is constant (Feijoo & Zouain, 1988). Based on the studies of Gomes *et al.* (2017) and Celis *et al.* (2020), the flow was modeled as turbulent, and the two-equation κ–ω SST model (Menter, 1994) was selected.

To determine the flow field, the time average conservation of mass and momentum were solved:

$$\frac{\partial u_j}{\partial x_j} = 0 \quad ; \quad \frac{\partial \rho u_j u_i}{\partial x_j} = -\frac{\partial \hat{p}}{\partial x_i} + \frac{\partial}{\partial x_j}\left[(\mu + \mu_t)\, 2\, S_{ij}\right] \quad \text{where} \quad S_{ij} = \frac{1}{2}\left(\frac{\partial u_i}{\partial x_j} + \frac{\partial u_j}{\partial x_i}\right) \tag{1}$$

where x_i represents coordinates axes, u_i the time average component of the velocity vector, ρ the density, μ the molecular viscosity, μ_t the turbulent viscosity and $\hat{p}$ is the modified pressure, which includes the turbulent dynamic pressure, dependent on the turbulent kinetic energy κ

$$\mu_t = \frac{\rho\, \kappa}{\omega} \xi_{\kappa-\omega} \quad ; \quad \hat{p} = p + \frac{2}{3}\, \rho\, \kappa \tag{2}$$

where $\xi_{\kappa-\omega}$ is a blending factor between the $\kappa - \varepsilon$ and $\kappa - \omega$ models, and ω is the turbulent energy dissipation. To complete the modeling, transport equations for κ and ω need also to be solved.

It was assumed that the inlet aortic valve was not deformed during the two years for the two patients, and the same uniform velocity normal to the inlet was imposed for both cases, considering the inlet turbulent intensity equal to 5% and the inlet specific dissipation length scale equal to the inlet valve diameter (Celis *et al*., 2020; Rojas-Solórzano et al., 2008). No slip condition was imposed at the aorta´s surface. Along the aorta, there is four outflow regions, where null diffusion was defined and a flow rate distribution was defined based on average values in the human body (Alastruey et al., 2016) as: 19.3% (brachiocephalic artery), 5.2% (left carotid artery), and 6.4% (left subclavian artery) and at the descending aorta the value was 69.1%.

Two viscosities were defined for the Newtonian fluid test cases: 3.5 cP and 7.2 cP. The selected non-Newtonian viscosity model was Carreau model (Shibeshi & Collins, 2005) and the viscosity is defined as

$$\mu = \mu_\infty + (\mu_0 - \mu_\infty)[1 + (\lambda\, \dot{\gamma})^2]^{\frac{n-1}{2}} \tag{3}$$

where μ_∞ is the viscosity at high strain rates, μ_0 is the lower limit corresponding to low strain rates, $\dot{\gamma} = \left(2\, S_{ij} S_{ij}\right)^{0.5}$ is the strain rate. λ and n are tunable model parameters. Here, the following values were defined as proposed by Cho & Kensey (1991): $\lambda = 3.313\ s$, $n = 0.3568$, $\mu_0 = 5.6$ cP and $\mu_\infty = 3.5$ cP.

The numerical solution was obtained with the software Fluent 2020 (ANSYS Inc.), based on the finite volume method (Patankar, 1980) with second-order Upwind discretization scheme for the spatial discretization of all equations. The solution was considered converged when the residuals of all discretized equations reached values inferior to 10^{-6}.

A grid test was performed and a mesh with 4×10^5 nodes was selected, since the difference of the pressure drop at the ascending aorta was inferior of 0.3% when the mesh size was doubled. Further it was guaranteed that the value of $y^+ = \rho\, y\, u_\tau / \mu$ of the first nodal point along the entire aorta surface was below 5, where $u_\tau = (\tau_w / \rho)^{0.5}$ and τ_w is the wall shear stress.

3. RESULTS AND DISCUSSION

To map the viscosity influence on hemodynamic patterns in the aneurysmatic aortas, the flow direction inside the aorta and the stress fields in the aortic wall were analyzed for two patients, considering the anatomy of their respective aortas

obtained from angiography exams, in two different years. For the first patient, the aneurysm presented growth, while for second, it did not. For each year and each patient, three cases were analyzed (i.e.: μ =7.2 cP; 3.5 cP and non-Newtonian model).

Figure 1 and Figure 2 illustrate the streamlines colored by turbulence kinetic energy (TKE). Through the analysis of both figures, it is possible to identify that in both years, for the two patients, with the three different viscosities, the flow is very similar, with the same main flow characteristics. It is noted how the blood flow impacts to the anterior wall region of the ascending aorta, and after the jet impact on the wall, the blood flow is directed to the aortic arch. However, smoother path lines are observed for patient 2 (Figure 2), who did not present aneurysm growth, as well as lower levels of turbulent kinetic energy. Also, because of the jet impact on the wall, it is observed for patient 1, for the higher viscosity case (Figs. 1a and 1d), a recirculation flow region in the vicinity of the posterior aortic wall. This recirculating flow is less visible for the lower viscosity case (Figs. 1b and 1e) case and for the non-Newtonian fluid (Figs. 1c and 1f).

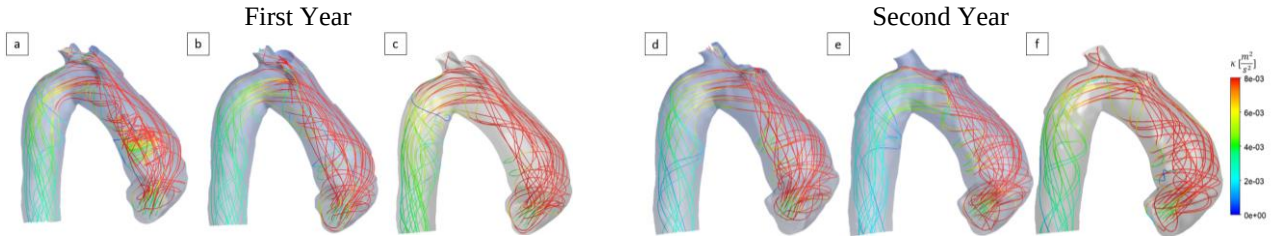

(a) 7.2 cP (b) 3.5 cP (c) Non-Newtonian (d) 7.2 cP (e) 3.5 cP (f) Non-Newtonian

Figure 1 - Streamlines colored by turbulent kinetic energy. Patient 1 – Aneurysm grew.

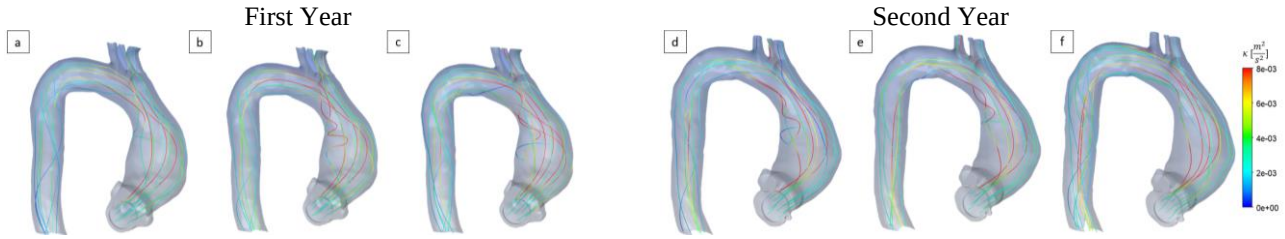

(a) 7.2 cP (b) 3.5 cP (c) Non-Newtonian (d) 7.2 cP (e) 3.5 cP (f) Non-Newtonian

Figure 2 - Streamlines colored by turbulent kinetic energy. Patient 2 – Aneurysm did not grow.

Figure 3 and Figure 4 present maps of the pressure distribution in the aortic wall, for the two patients. It can be seen that this variable has a small dependence on the viscosity field. The observed recirculation region at the posterior aortic wall of patient 1, with the high viscosity model, lead to a less pronounced pressure at the impact region (Figure 3). However, for all viscosity models, for patient 1, who presented aneurysm growth, one can clearly see the increase of the pressure level at the jet impingement region in the second year. With respect to patient 2 (Figure 4), without aneurysm growth, equivalent pressure distribution was obtained for the three viscosities cases. Further, lower and uniform level of pressure at the ascending aortic wall was obtained, a characteristic also observed by Almeida *et al.* (2021).

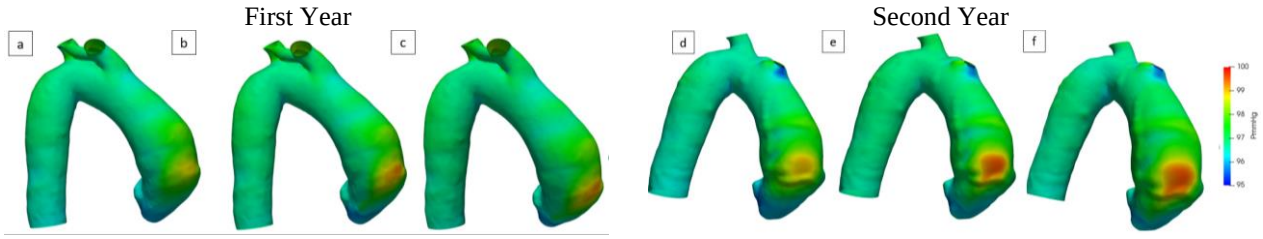

(a) 7.2 cP (b) 3.5 cP (c) Non-Newtonian (d) 7.2 cP (e) 3.5 cP (f) Non-Newtonian

Figure 3 - Wall pressure. Patient 1 – Aneurysm grew.

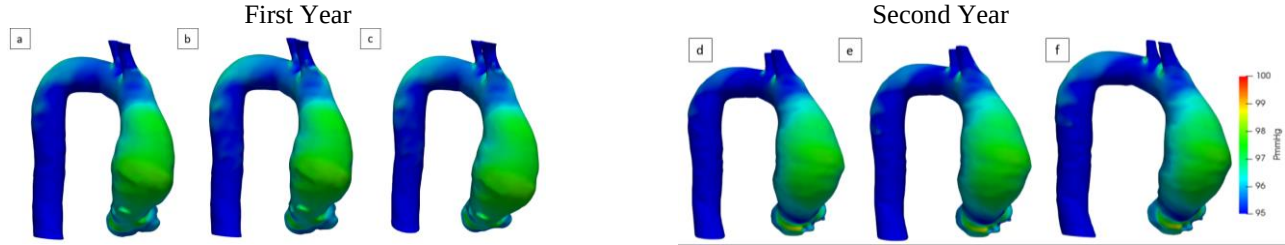

(a) 7.2 cP (b) 3.5 cP (c) Non-Newtonian (d) 7.2 cP (e) 3.5 cP (f) Non-Newtonian

Figure 4 - Wall pressure. Patient 2 – Aneurysm did not grow.

Figure 5 and Figure 6 show, for each patient, the Wall Shear Stress (WSS) field obtained from each of the three viscosities cases analyzed. Once again, the overall distribution is equivalent for both patient and for all viscosities, since the blood jet after impinging at the aortic flow is deflected and flows along is arch, leading to an increase of the WSS, resulting in equivalent locations of high and low WSS. However, the viscosity influence is larger for this variable, and higher WSS are observed for both patients for the high viscosity case (a and d), but the WSS distribution for the low viscosity cases (b and e) are extremely similar to the non-Newtonian cases (c and f). Analyzing both figures, can be notice the larger level of WSS for the patient who presented aneurysm growth.

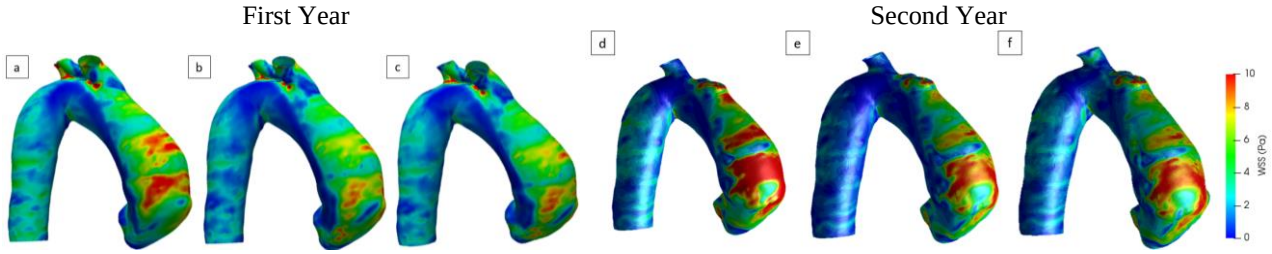

(a) 7.2 cP (b) 3.5 cP (c) Non-Newtonian (d) 7.2 cP (e) 3.5 cP (f) Non-Newtonian

Figure 5 - Wall shear stress, WSS. Patient 1 – Aneurysm grew.

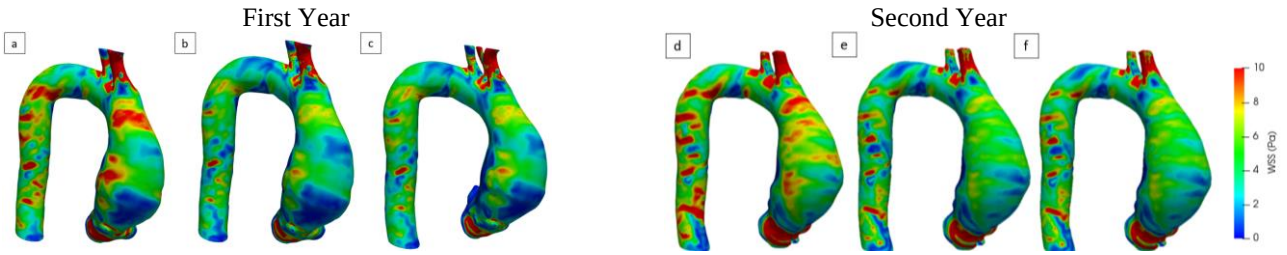

(a) 7.2 cP (b) 3.5 cP (c) Non-Newtonian (d) 7.2 cP (e) 3.5 cP (f) Non-Newtonian

Figure 6 - Wall shear stress, WSS. Patient 2 – Aneurysm did not grow.

Analyzing Figure 3 through Figure 6, it was possible to make an initial assessment regarding the viscosity influence on the wall pressure and WSS, however to perform a deeper evaluation, it was calculated the variation coefficient (VC) (Everitt & Skrondal, 2002) of pressure and WSS. Through the VC it is possible to quantify the viscosity effect in each point cell (i) of the aortic wall. The μ =3.5 cP case is used as a base case in order to determine the VC of pressure and WSS, i.e.: a comparison of high viscosity vs low viscosity is presented, followed by a comparison of Newtonian μ =3.5 cP vs non-Newtonian cases. The variation coefficient of pressure and WSS is determined according to

$$VC_{\phi}^{3.5\times7.2} = \left(\frac{\sigma_{i_\phi}}{\bar{\phi}_i}\right) \times 100 \quad ; \quad \sigma_{i_\phi} = \sqrt{\frac{(\phi_{i,3.5}-\bar{\phi}_i)^2+(\phi_{i,7.2}-\bar{\phi}_i)^2}{2}} \quad ; \quad \bar{\phi}_i = \frac{\phi_{i,3.5}+\phi_{i,7.2}}{2} \tag{4}$$

$$VC_{\phi}^{3.5\times NN} = \left(\frac{\sigma_{i_\phi}}{\bar{\phi}_i}\right) \times 100 \quad ; \quad \sigma_{i_\phi} = \sqrt{\frac{(\phi_{i,3.5}-\bar{\phi}_i)^2+(\phi_{i,\mathrm{NN}}-\bar{\phi}_i)^2}{2}} \quad ; \quad \bar{\phi}_i = \frac{\phi_{i,3.5}+\phi_{i,NN}}{2} \tag{5}$$

Figure 7 shows the $VC_p^{3.5\times7.2}$ distribution for the first year and second year of the aorta of both patients, while Figure 8 illustrates the $VC_p^{3.5\times NN}$. The pressure variation was so small that a logarithmic scale was employed to aid in the visualization of the differences. When comparing cases 3.5 cP to 7 cP, it is noted that the regions where the viscosity variation had the greatest influence (less than 1%) were in a small region at the beginning of the ascending aorta, in the aortic arch and in the descending aorta. In most of the ascending aorta, the viscosity influence on the pressure field was between 0.01% and 0.1%. Even smaller pressure variations were obtained between the 3.5cP Newtonian and non-Newtonian cases, with $VC_p^{3.5\times NN}$ values smaller that 0.01% in almost all the aortic domain evaluated.

The impact of the viscosities in the WSS distribution is shown in Figure 9 and Figure 10 through the distribution of $VC_{WSS}^{3.5\times7.2}$ and $VC_{WSS}^{3.5\times NN}$ at the aortic wall for both patients and years. The influence of viscosity variation from 3.5 cP to 7 cP on the WSS field (Figure 9) leads to $VC_{WSS}^{3.5\times7.2}$ values equal or greater than 50% in regions located especially in the descending aorta and aortic arch. It is interesting to mention that the regions with a high viscosity influence are characterized by being those with a smaller aortic diameter and accentuated aortic curvature. However, in the aneurysmatic region of the ascending aorta, the viscosity influence on the WSS was mostly around 20%. Figure 10 refers to the $VC_{WSS}^{3.5\times NN}$, and in this case the non-Newtonian viscosity influences less than 10 % in almost all the WSS field. Again, the regions of more WSS variation are located around the smaller aortic diameter and accentuated aortic curvature.

Patient 1 – Aneurysm grew Patient 2 – Aneurysm did not grow

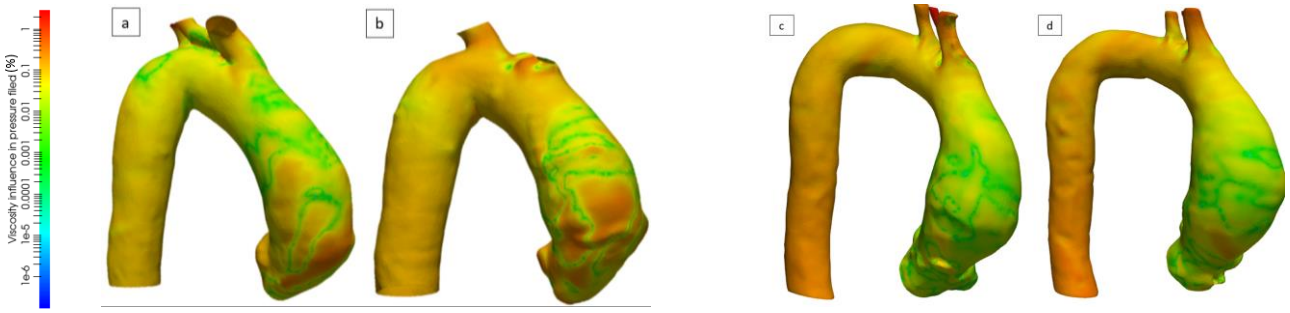

(a) First Year (b) Second Year (c) First Year (d) Second Year

Figure 7 – Influence of Newtonian viscosity 3.5cP × 7.2 cP in wall pressure, $VC_p^{3.5\times7.2}$.

Patient 1 – Aneurysm grew Patient 2 – Aneurysm did not grow

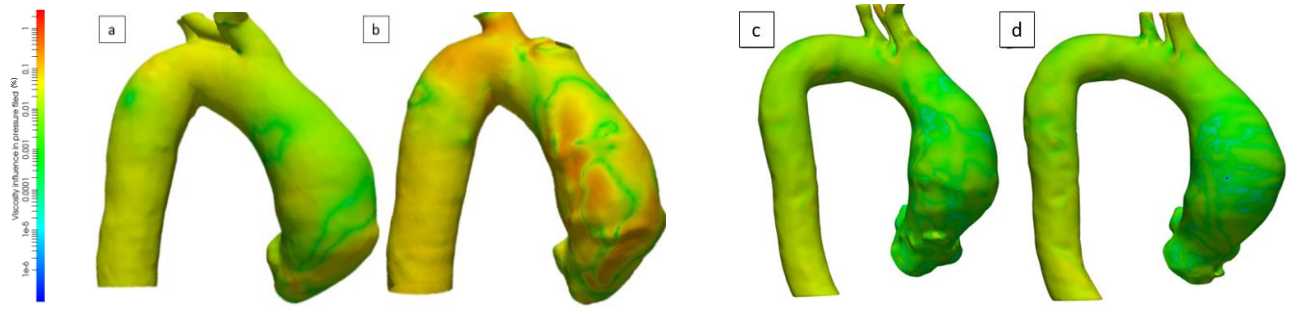

(a) First Year (b) Second Year (c) First Year (d) Second Year

Figure 8 – Influence of Newtonian viscosity 3.5cP × non Newtonian viscosity in wall pressure, $VC_p^{3.5\times NN}$.

Patient 1 – Aneurysm grew Patient 2 – Aneurysm did not grow

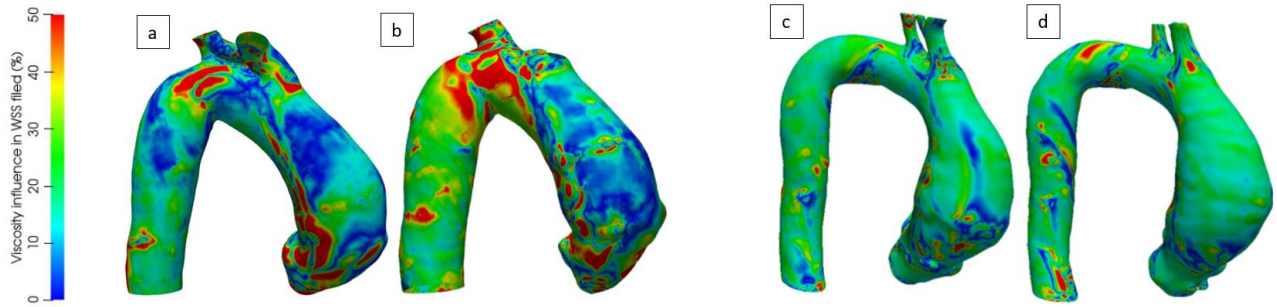

(a) First Year (b) Second Year (c) First Year (d) Second Year

Figure 9 – Influence of Newtonian viscosity 3.5cP × 7.2 cP in WSS, $VC_{WSS}^{3.5\times7.2}$.

Patient 1 – Aneurysm grew Patient 2 – Aneurysm did not grow

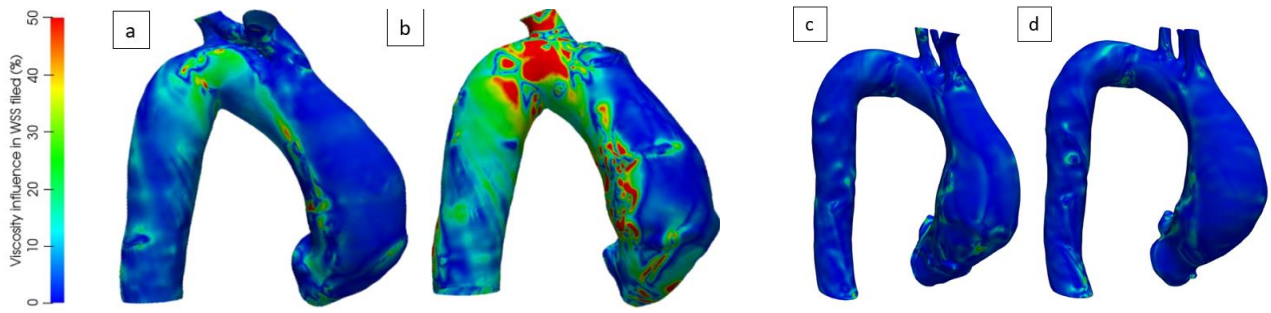

(a) First Year (b) Second Year (c) First Year (d) Second Year

Figure 10 - Influence of Newtonian viscosity 3.5cP × non Newtonian viscosity in WSS, $VC_{WSS}^{3.5\times NN}$.

Figure 11 shows the non-Newtonian viscosity field in all the aortic internal domain. Through the analysis of Figure 11 it is revealed that in most of the internal aortic domain the non-Newtonian viscosity maintains its magnitude order close to that of the Newtonian viscosity (3.5 cP). Especially near to the aortic wall the value of the non-Newtonian viscosity is practically equal to the Newtonian viscosity. The previous line of reasoning explains why the pressure and WSS resulting from the non-Newtonian case were so close to those obtained from the Newtonian 3.5 cP case.

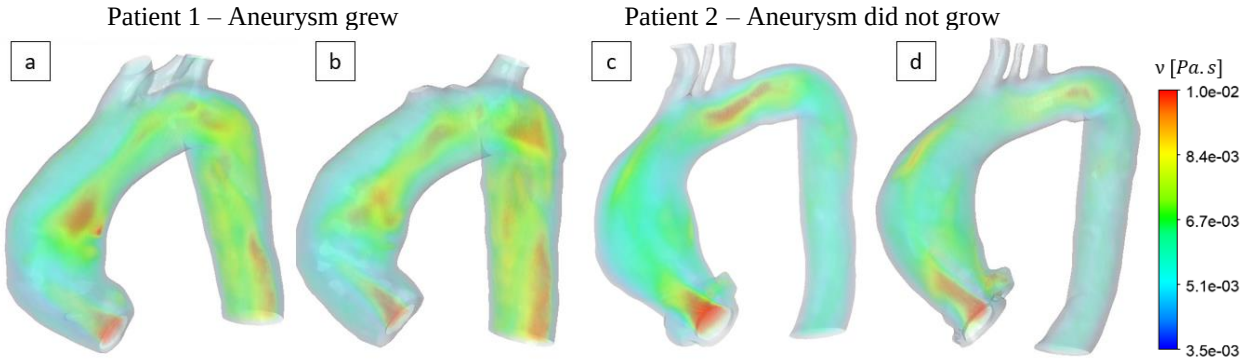

(a) First Year (b) Second Year (c) First Year (d) Second Year

Figure 11 - Non-Newtonian viscosity field. First Year.

4. CONCLUSIONS

The influence of the viscosity in the flow pattern and tension distribution at the ascending aorta of patients with aneurysm was examined. Two patients were investigated, by examining the flow pattern and by comparing the evolution of the pressure and WSS between two years. One patient presented aneurysm growth and the other did not. The blood was modelled as a Newtonian fluid, with two different viscosities, and as a non-Newtonian fluid, described with Carreau model. All cases presented very similar results, and the same interpretation regarding the impact of the flow for the two different patients was obtained. Smoother streamlines were seen for the patient without aneurysm growth, with not only lower TKE level inside the aorta, but lower wall pressure and WSS, than the patient who presented aneurysm growth. It was verified that the results of pressure were quite similar for all viscosities models. A slightly more complex flow structure was obtained for the 7.2 cP viscosity case, with also a slightly larger WSS. The results for 3.5cP viscosity cases were almost equal to the Non-Newtonian cases, not only because the limiting Carreau viscosity was the same, but due to the fact that the aorta is a vessel with a very large diameter, with small impact of the deformation rate.

5. ACKNOWLEDGEMENT

This work was supported by the Cardiovascular Engineering Laboratory PUC-Rio. The authors also thank the Brazilian government agencies CNPq and CAPES for the continuous support.

6. REFERENCES

Alastruey, J., Xiao, N., Fok, H., Schaeffter, T., & Figueroa, C. A.,2016. "On the impact of modelling assumptions in multi-scale, subject-specific models of aortic haemodynamics". *Journal of The Royal Society Interface*, Vol. 13, No.119, p. 20160073.

Almeida, G. C., Azevedo, B. A., Azevedo, F. S., Kalaoun, K., Ibanez, I., Teixeira, P. S., Gottieb, I., Nelo, M.M., Oliveira, G.M.M. and Nieckele, A. O., 2021. "Computational Fluid Dynamics to Access the Future Risk of Ascending Aortic Aneurysms". *Arquivos Brasileiros de Cardiologia*, in press.

Becsek, B., Pietrasanta, L., & Obrist, D., 2020. "Turbulent Systolic Flow Downstream of a Bioprosthetic Aortic Valve: Velocity Spectra, Wall Shear Stresses, and Turbulent Dissipation Rates". *Frontiers in Physiology*, Vol. 11, p. 577188.

Bessa, G. M., Fernandes, L. S., Gomes, B. A. A., & Azevedo, L. F. A., 2021. "Influence of aortic valve tilt angle on flow patterns in the ascending aorta". *Experiments in Fluids*, Vol. 62, No.5, p. 113.

Celis, D., Gomes, B. A. de A., Ibanez, I., Azevedo, P. N., Teixeira, P. S., & Nieckele, A. O., 2020. "Predição do Mapa de Estresse em Aorta Ascendente: Otimização da Posição Coaxial no Implante Valvar Aórtico Percutâneo". *Arquivos Brasileiros de Cardiologia*,Vol. 115, No.4, pp.680–687.

Cho, Y., & Kensey, K., 1991. "Effects of the non-Newtonian viscosity of blood on flows in a diseased arterial vessel". Part 1: Steady flows. *Biorheology*, Vol. 28, No. 3-4, pp. 241–262.

Crowley, T. A., & Pizziconi, V.,2005. "Isolation of plasma from whole blood using planar microfilters for lab-on-a-chip applications". *Lab on a Chip*, Vol. 5. No.9, pp. 922–929.

Everitt, B., & Skrondal, A., 2010. *The Cambridge dictionary of statistics*. Cambridge, UK. Cambridge University Press.

Feijoo, R. A., & Zouain, N., 1988. "Formulations in rates and increments for elastic-plastic analysis". *International Journal for Numerical Methods in Engineering*, Vol. 26, No.9, pp. 2031–2048.

Gomes, B. A. de A., Camargo, G. C., dos Santos, J. R. L., Azevedo, L. F. A., Nieckele, Â. O., Siqueira-Filho, A. G., & de Oliveira, G. M. M.,2017. "Influência do ângulo de Lnclinação da prótese percutânea aórtica no campo de velocidade e estresse de cisalhamento". *Arquivos Brasileiros de Cardiologia*, Vol. 109, No.3, pp.231–240.

Ibanez, I. F., de Azevedo Gomes, B. A., & Nieckele, A. O., 2020. "Effect of percutaneous aortic valve position on stress map in ascending aorta: A fluid-structure interaction analysis". In *Artificial Organs*, Vol 00, pp. 1-12.

Johnson, E. L., Wu, M. C. H., Xu, F., Wiese, N. M., Rajanna, M. R., Herrema, A. J., Ganapathysubramanian, B., Hughes, T. J. R., Sacks, M. S., & Hsu, M.-C., 2020. "Thinner biological tissues induce leaflet flutter in aortic heart valve replacements". *Proceedings of the National Academy of Sciences*, Vol. 117, No.32, pp.19007-19016.

Long, D. S., Smith, M. L., Pries, A. R., Ley, K., & Damiano, E. R., 2004. "Microviscometry reveals reduced blood viscosity and altered shear rate and shear stress profiles in microvessels after hemodilution". *Proceedings of the National Academy of Sciences of the United States of America*, Vol. 101, No.27, pp.10060–10065.

Menter, F. R., 1994. "Two-equation eddy-viscosity turbulence models for engineering applications". *AIAA Journal*, Vol. 32, No.8, pp.1598–1605.

Patankar, S. V.,1980. *Numerical heat transfer and fluid flow*. Hemisphere Publishing Corporation.

Rojas-Solórzano, L., Salazar, F., & Antaki, J., 2008. "Numerical Study of Turbulence Models in the Computation of Blood Flow in Cannulas". *Proceedings of the ASME 2008 Fluids Engineering Division Summer Meeting collocated with the Heat Transfer, Energy Sustainability, and 3rd Energy Nanotechnology Conferences. Volume 1: Symposia, Parts A and B*. Jacksonville, Florida, USA. August 10–14, pp. 999-1005.

Shibeshi, S. S., & Collins, W. E., 2005. "The Rheology of Blood Flow in a Branched Arterial System". *Applied Rheology*, Vol. 15, No. 6, pp. 398–405.

Viscardi, F., Vergara, C., Antiga, L., Merelli, S., Veneziani, A., Puppini, G., Faggian, G., Mazzucco, A., & Luciani, G. B., 2010. "Comparative finite element model analysis of ascending aortic flow in bicuspid and tricuspid aortic valve". *Artificial Organs*, Vol. 34 ,No.12, pp. 1114–1120.

Yamamoto, H., Yabuta, T., Negi, Y., Horikawa, D., Kawamura, K., Tamura, E., Tanaka, K., & Ishida, F., 2020. "Measurement of human blood viscosity a using Falling Needle Rheometer and the correlation to the Modified Herschel-Bulkley model equation". *Heliyon*, Vol. 6, No. 9, e04792.

7. RESPONSIBILITY NOTICE

The authors are the only responsible for the printed material included in this paper.